

RESSALVA

Atendendo solicitação do(a)
autor(a), o texto completo desta tese
será disponibilizado somente a partir
de 04/10/2018.

UNIVERSIDADE ESTADUAL PAULISTA
CAMPUS DE ARARAQUARA
PROGRAMA DE PÓS-GRADUAÇÃO EM QUÍMICA

Bacterial cellulose and silk fibroin biopolymers: Biotemplates to design nanostructured materials for optical applications.

MOLÍRIA VIEIRA DOS SANTOS

Ph.D thesis

2016

MOLÍRIA VIEIRA DOS SANTOS

Biopolímeros de celulose bacteriana e fibroína da seda: biotemplates para a preparação de materiais nanoestruturados para aplicações ópticas

Tese apresentada ao Instituto de Química,
Universidade Estadual Paulista,
como parte dos requisitos para obtenção
do título de Doutor em Química.

Orientador: Prof. Dr. Sidney José Lima Ribeiro.

Araraquara

2016

FICHA CATALOGRÁFICA

| | |
|-------|--|
| S237b | <p>Santos, Molíria Vieira dos</p> <p>Bacterial cellulose and silk fibroin biopolymers: biotemplates to design nanostructured materials for optical applications = Biopolímeros de celulose bacteriana e fibroína da seda: biotemplates para a preparação de materiais nanoestruturados para aplicações ópticas / Molíria Vieira dos Santos. – Araraquara: [s.n.], 2016 163 p.: il.</p> <p>Tese (doutorado) – Universidade Estadual Paulista, Instituto de Química Orientador: Sidney José Lima Ribeiro</p> <p>1. Biopolímeros. 2. Cristais líquidos. 3. Sílica. 4. Luminescência. 5. Laser em física. I. Título.</p> |
|-------|--|

MOLÍRIA VIEIRA DOS SANTOS

Bacterial cellulose and silk fibroin biopolymers: Biotemplates to design nanostructured materials for optical applications.

Thesis presented to the Institute of Chemistry,
São Paulo State University “Júlio de Mesquita Filho”,
to obtain the Ph.D in Chemistry.

Advisor: Prof. Dr. Sidney José Lima Ribeiro.

Araraquara

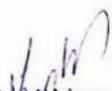
2016

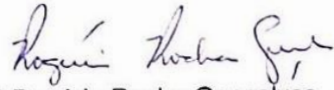
MOLÍRIA VIEIRA DOS SANTOS

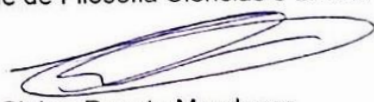
Tese apresentada ao Instituto de Química, Universidade Estadual Paulista, como parte dos requisitos para obtenção do título de Doutora em Química.

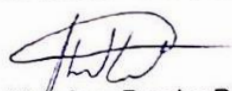
Araraquara, 04 de outubro de 2016.

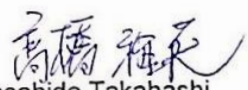
BANCA EXAMINADORA


Prof. Dr. Sidney José Lima Ribeiro (Orientador)
Instituto de Química – UNESP, Araraquara - SP


Profª Drª Rogéria Rocha Gonçalves
Faculdade de Filosofia Ciências e Letras – USP, Ribeirão Preto - SP


Prof. Dr. Cleber Renato Mendonça
Instituto de Física – USP, São Carlos - SP


Prof. Dr. Ubirajara Pereira Rodrigues Filho
Instituto de Química – USP, São Carlos -SP


Prof. Dr. Masahide Takahashi
Faculdade Osaka Prefecture University – Osaka, Japão

1. DATA

MOLÍRIA VIEIRA DOS SANTOS

- 1.1. Date of birth: 04/29/1986
- 1.2. Nationality: Brazilian
- 1.3. Citizenship: Poços de Caldas
- 1.6. Profession: Chemist
- 1.7. E-mail: moliria.santos@gmail.com

2. ACADEMIC EDUCATION

- 2.1. Bachelor in chemistry – State of São Paulo University “Júlio de Mesquita Filho” (UNESP/Araraquara) – 2010.
- 2.2. Master in chemistry – State of São Paulo University “Júlio de Mesquita Filho” (UNESP/Araraquara) – 2012.

3. BIBLIOGRAPHIC PRODUCTION

3.1. Presentations in conferences: 13 international and 9 national.

3.2. Extended abstracts published in conference proceedings:

1) SANTOS, M. V.; TOLENTINO, C.; RIBEIRO, S.; BARUD, H.; DE ARAUJO, C. B.; GOMES, A.; DE MELO, L. **Biopolymer Random Laser Consisting of Rhodamine 6G and Silica Nanoparticles Incorporated to Bacterial Cellulose**. In: Conference on Lasers and Electro-Optics 2012. Washington: OSA, 2012. p. JW4A.51.

2) SILVA, R. R.; TOLENTINO, C.; SANTOS, M. V.; MELO, L.; RIBEIRO, S. J. L.; ARAUJO, C. B.; GOMES, A.; BARBOSA-SILVA, R. **Efficient Distributed Feedback Dye Laser in Silk Fibroin Films**. In: Conference on Lasers and Electro-Optics 2012. Washington: OSA, 2012. p. JW4A.53.

3.3. Publications in journals:

1) CAIUT, J. M. A.; BARUD, H.; SANTOS, M.; Oliveira U. L.; MENEZES, J. F. S.; MESSADDEQ, Y.; RIBEIRO, S. J. L. Luminescent multifunctional biocellulose membranes. **Proceeding SPIE**, v. 8104, p. 81040Z-1-81040Z-9, 2011.

2) MARQUES, L. F.; DOS SANTOS, M. V., RIBEIRO, S. J. L., CASTELLANO, E. E.; MACHADO, F. C. Terbium (III) and dysprosium (III) 8-connected 3D networks containing 2,5-thiophenedicarboxylate anion: Crystal structures and photoluminescence studies. **Polyhedron**, v. 38, p. 149 - 156, 2012.

3) SANTOS, M. V., DOMINGUEZ, C. T., SCHIAVON, J. V.; BARUD, H. S.; MELO, L. A., RIBEIRO, S. J. L.; GOMES, A. S. L.; ARAÚJO, C. B. Random laser action from flexi biocellulose-based device. **Journal of Applied Physics**, v. 115, p. 083108, 2014.

- 4) SILVA, R. R.; DOMINGUEZ, C. T.; SANTOS, M. V.; BARBOSA-SILVA, R.; CAVICCHIOLI, M.; CHRISTOVAN, L. M., DE MELO, L. S. A., GOMES, ANDERSON S. L., DE ARAÚJO, CID B., RIBEIRO, SIDNEY J. L. Silk fibroin biopolymer films as efficient hosts for DFB laser operation. **Journal of Materials Chemistry C**, v. 1, p. 7181, 2013.
- 5) MARQUES, L. F.; CORRÊA, C. C.; DA SILVA, R. R., DOS SANTOS, M. V.; RIBEIRO, S. J. L.; MACHADO, F. C. Structure, characterization and near-infrared emission of a novel 6-connected uninodal 3D network of Nd(III) containing 2,5-thiophenedicarboxylate anion. *Inorganic Chemistry Communications*, v. 37, p. 66 - 70, 2013.
- 6) RIBEIRO, S. J.L.; DOS SANTOS, M. V.; SILVA, R. R.; PECORARO, É.; GONÇALVES, R. R.; CAIUT, J. M. A. (2015) Optical Properties of Luminescent Materials, in **The Sol-Gel Handbook - Synthesis, Characterization, and Applications: Synthesis, Characterization and Applications**, 3-Volume Set (eds D. Levy and M. Zayat), Wiley-VCH Verlag GmbH & Co. KGaA, Weinheim, Germany. doi: 10.1002/9783527670819.ch30
- 7) LIMA, L. R.; SANTOS, D. B.; SANTOS, M. V.; BARUD, H. S.; HENRIQUE, M. A.; PASQUINI, D.; PECORARO, E.; RIBEIRO, S. J. L.; Cellulose nanocrystals from bacterial cellulose. **Química Nova**, v. 38, n. 9, p. 1140 - 1147, 2015.
- 8) MARQUES, L. F., CUIN, A. C.; GUSTAVO S.G., SANTOS, M. V., RIBEIRO, S.J.L.; MACHADO, F. C. Energy Transfer process in highly photoluminescent binuclear hydrocinnamate of europium, terbium and gadolinium containing 1,10-phenanthroline as ancillary ligand. **Inorganica Chimica Acta**, v. 441, p. 67 - 77, 2015.
- 9) GONÇALVES, L. P.; FERREIRA-NETO, E. P.; ULLAH, S.; SOUZA, L. V. Y.; ORLANDO A. E.; SANTOS, M. V.; RIBEIRO, S. J. L.; R-F, U. PEREIRA Enhanced photochromic response of ormosil-phosphotungstate nanocomposite coatings doped with TiO₂ nanoparticles. **Journal of Sol-Gel Science and Technology**, v. 76, p. 386 - 394, 2015.
- 10) NIGOGHOSSIAN, K.; SANTOS, M. V.; BARUD, H.S.; SILVA, R. R., ROCHA, L.A.; CAIUT, J. M. A.; ASSUNÇÃO, R. M. N., SPANHEL, L. P. M.; MESSADDEQ, Y. RIBEIRO, S.J.L. Orange pectin mediated growth and stability of aqueous gold and silver nanocolloids. **Applied Surface Science**, v. 341, p. 28 - 36, 2015.
- 11) MARQUES, L. F.; CORREA, C. C.; RIBEIRO, S. J.L.; SANTOS, M. V.; DUTRA, JOSÉ D. L.; FREIRE, R. O.; MACHADO, F. C. Synthesis, structural characterization, luminescent properties and theoretical study of three novel lanthanide metal-organic frameworks of Ho(III), Gd(III) and Eu(III) with 2,5-thiophenedicarboxylate anion. **Journal of Solid State Chemistry**, v. 227, p. 68 - 78, 2015.
- 12) RIBEIRO, S. J. L.; SILVA, R. R.; SALVI, D. T. B.; SANTOS, M. V.; BARUD, H. S; MARQUES, L. F.; SANTAGNELI, S. H.; TERCJAK, A. Multifunctional organic-inorganic hybrids based on cellulose acetate and 3-glycidoxypropyltrimethoxysilane. **Journal of Sol-Gel Science and Technology**. doi:10.1007/s10971-016-4089-x.
- 13) SILVA, D. L. C.; KASSAB, L. R. P.; MARTINELLI, J. R.; SANTOS, A. D., RIBEIRO, S. J. L.; SANTOS, M. V. Characterization of thin carbon films produced by the magnetron sputtering technique for optoelectronics and photonics applications. **Material Research**. doi: 10.1590/1980-5373-MR-2015-0058.

I dedicate this thesis to my best friend and husband Igor,
who I admire and love for his kindness and honor.

“The mind that opens up to a new idea never returns to its original size.”

Albert Einstein

ACKNOWLEDGEMENTS

My advisor likes to spread during our work in the lab “You should enjoy your work and everything gonna be all right”. Surely, the development of this PhD research yielded me many good results, which were only achieved thanks to the living together and collaboration of a number of people and institutions. However, sometimes I had hard times and all my love for chemistry helped me to overcome and reach the end.

I am glad of had been advised by Prof. Dr. Sidney José Lima Ribeiro, who I admire for his expertise, enthusiasm and promptitude. I am deeply grateful for all support, guidance and opportunities, which were essentials to my progress.

Prof. Dr. Edison Pecoraro has also been an important person during all my graduation. Thank you for teaching me each step in the optical lab, for the valuable discussions and for helping me with my questions about the experiments.

I have many reasons to acknowledge my dear friend Prof. Dr. Hernane da Silva Barud, but the one I am must thankful is for his guidance during my undergrad, for teaching me since the start, points of experimental science and for encourage my career. Thanks also to Prof. Dr. Agnieszka Terjak and Dr. Juncal Guitierrez for help me with part of my work in this thesis.

My gratitude to the whole Photonics Materials Group: Professor Dr. Marcelo Nalin, Dr. Silvia Helena Stagnelli, Dr. Mauricio Cavichioli, Dr. Danilo Manzani and Ferminio Cesar Polachini; and especially to my labmates, including the former generation, Robson and Rafael; my contemporaneous, Lippy, Denise and Leandro; and also to the youngers Camila, Lais, Karina, Gustavo, Lais Galvão, Andréia, Mariana, Thais, Lívia and Tércio. Thank you all for the help in several points, for the pleasurable working hours and for the quality interaction.

I would like to thanks Prof. Dr. Anderson S. L. Gomes and Prof. Dr. Cid B. de Araújo and their students Dr. André L. Moura and Dr. Vlademir Jerez, from Universidade Federal de Pernambuco - Recife, for had been my collaborators, providing investigation of random laser action of the silica monoliths synthesized in this thesis.

I really appreciate the opportunity of had worked in Aveiro University, through the partnership with Prof. Dr. Luis Dias Carlos and Prof. Dr. Maria Rute Sá Amorin Ferreira André, by which I could expand my knowledge to the luminescence and optical materials get in touch with many interesting people. Thank you to the whole Luis’s Group for the help and hospitality. Concerning my stay in Aveiro, I never thought I would meet some of my dear friends at Aveiro

University. Thanks Sangeetha, Cyntia, Denis, Vânia and Sandra for the friendship and protection abroad.

I would like to express my appreciation to my family, my husband Igor and his family, especially to my mom Inez and my sisters Flávia and Patrícia, even with all its simplicity they provided me the chance to get here. Also, my appreciation to the new family members Crystian, Ícaro and Pedro, who I love with all heart.

Finally, my acknowledgments to São Paulo State University - Araraquara – through Institute of Chemistry – that has held all my studies since the beginning of my undergrad in 2006. I am finishing a 10-year process, which definitely changed my perspectives. And to São Paulo Research Foundation (FAPESP) for the financial support in all those steps, manly for the grants of my scholarship: 2014/12424-2.

ABSTRACT

Among all natural polymers, bacterial cellulose and silk fibroin offer unlimited opportunities for processing, functionalization, and biological integration. This thesis presents the preparation and characterization of nanostructured materials based on bacterial cellulose produced by *Gluconacetobacter xylinus* bacteria, as well as regenerated silk fibroin stemmed from the cocoons of silkworms (*Bombyx mori*) for optical applications.

Firstly, dried bacterial cellulose membranes were utilized to prepare cellulose nanocrystals (CNC). CNC were casted in the form of thick iridescent films whose color originates in the periodic patterning of layers in a chiral nematic texture created by self-assembly of rod crystallites. Once the CNC films were obtained, self-sustainable films were coated with a low molecular weight nematic liquid crystal (LC), 4'-(hexyloxy)-4-biphenylcarbonitrile (HOBC). The materials were obtained as free-standing iridescent films, with chiral nematic structure that exhibited modulated optical properties, in response to external stimulus, such as thermal gradient or relatively small electrical voltage. The scanning electron microscopy (SEM) confirmed that the composite film structure comprises the multi-domain Bragg reflectors. The relationship between the surface structure and thermo-responsive properties of investigated HOBC coated with CNC film was examined using transmission optical microscopy (TOM). Additionally, electrostatic force microscopy (EFM) measurement was employed to prove the effect of external stimuli, in this case applied voltage, on the HOBC liquid crystal coated with CNC film.

The second part of this thesis involves the design of luminescent iridescent films through the combination of CNC suspension with tetraethoxysilane (TEOS) and ethanolic solutions of Rhodamine 6G (Rh6G). These materials were obtained as freestanding composite films with chiral nematic organization. The optical properties of such films can be tuned through changes in the silica/CNC proportion during the preparations. Photoluminescence measurements, as function of the detection angle, were realized in order to investigate the influence of photonic structure in the light emission of composite films. Our findings demonstrated that the photonic structure of the film acts as an inner- filter, causing selective suppression of the light emitted with a variation of the detection angle. This behavior was found to be dependent of the bandgap position on the photonic structure of these materials.

Lastly, we designed structured organic-inorganic hybrids (OIH) based on silica and silk fibroin. The materials were obtained as robust monoliths possessing different fibroin fractions. The SEM images demonstrated in-situ self-assembly of fibroin nanofibers dispersed into the

IOH monoliths. Structural characterization of OIH monoliths was performed by Raman and solid state NMR spectroscopies. Our findings demonstrated that precipitated fibroin presented prevailing β -sheet conformation. Furthermore, we demonstrated that the fibroin nanofibers can be used as biotemplates, acting as a sacrificial material to development porous silica monoliths. The porous silica monoliths doped with rhodamine 6g (Rh6G) exhibited efficient RL action with low threshold power excitation and narrowing linewidth. From the spectral behavior, it is inferred that the RL operates in the diffusive regime in hierarchical macro–mesoporous network. In addition, analysis of the emission spectra showed two gain mechanisms coupled, specifically the random lasing and the stimulated Raman scattering, which suggest that designed materials can also be promising for random Raman laser applications.

Keywords: bacterial cellulose, silk fibroin, cellulose nanocrystals, nematic liquid crystal, silica, organic-inorganic hybrids, photonic devices and random lasers.

RESUMO

Entre os polímeros naturais, celulose bacteriana e fibroína da seda oferecem inúmeras oportunidades para funcionalização, processamento e integração biológica. Esta tese apresenta a preparação e caracterização de novos materiais nanoestruturados para aplicações ópticas utilizando celulose bacteriana produzida pela bactéria *Gluconacetobacter xylinus*, como também em fibroína regenerada extraída de casulos do bicho da seda (*Bombyx mori*).

Primeiramente, membranas de celulose bacteriana secas foram utilizadas para a preparação de nanocristais de celulose (NCC). Os nanocristais de celulose foram processados na forma de filmes espessos e iridescentes nos quais a cor tem origem de padrões periódicos de camadas em uma estrutura nemática quiral criada pelo alto montagem dos bastões cristalinos. Uma vez obtido o filme de NCC, o mesmo foi revestido com um cristal líquido nemático de baixo peso molecular, 4'- (hexiloxi) - 4 - bifenilcarbonitrila (HOBC). O material foi obtido como um filme auto-suportado, iridescente, formado por uma estrutura nematic quiral e que exhibe moduladas propriedades em resposta a estímulos externos, tais como, gradiente de temperatura e relativa pequena voltagem elétrica. Imagens de microscopia eletrônica de varredura (MEV) confirmaram a estrutura do filme formada por múltiplos domínios refletoras de Bragg. A relação entre a estrutura da superfície e as propriedades de resposta térmica do revestimento de HOBC no filme foram investigadas utilizando microscopia óptica de transmissão (TOM). Além disso, medidas de microscopia de força eletrostática foram empregadas para provas o efeito do estímulo externo, neste caso da voltagem aplicada, no revestimento de cristal líquido HOBC no filme.

A segunda parte desta tese envolve a preparação de filmes iridescente luminescentes através da combinação da suspensão de NCC com tetraetoxisilano (TEOS) e uma solução etanólica de rodamina 6G (Rh6G). Estes materiais foram obtidos como filmes compósitos auto suportados com ordenação nemática quiral. As propriedades ópticas dos filmes foram sintonizadas através de mudanças na proporção de sílica/NCC na preparação. Medidas de fotoluminescência em função do ângulo foram realizadas a fim de investigar a influência da estrutura fotônica com ordenação nemática quiral na emissão de luz pelos filmes compósitos. Os resultados demonstraram que a estrutura fotônica dos filmes atuam como um filtro interno causando supressão seletiva da luz emitida com a variação do ângulo de detecção. Este comportamento mostrou-se dependente da posição da banda proibida destes materiais.

Por fim, nós preparamos híbridos orgânico - inorgânicos (HOI) baseados em sílica e fibroína da seda. Os materiais foram obtidos em forma de monolitos robustos cont

diferentes concentrações de fibroína. As imagens de MEV apresentam a precipitação de nanofibras de fibroína dispersas dentro dos HOIs. A caracterização estrutural das amostras foi realizada por espectroscopia Raman e ressonância magnética nuclear (RMN) do estado sólido. Os resultados demonstraram que a fibroína precipitada apresenta preferencial conformação folha- β . Nós demonstramos ainda que as nanofibras de fibroína podem ser utilizadas como moldes, atuando com um material de sacrifício para a produção de monolitos de sílica porosos. Os monolitos de sílica porosa dopados com rodamina 6G (Rh6G) exibiram eficiente ação laser aleatório (LA), com baixo limiar laser e estreita largura de banda. A partir do comportamento espectral, infere-se que o LA opera no regime difusivo na rede hierarquia formada por macro e mesoporos. Além deste comportamento, através de análise do espectro de emissão foi observado o acoplamento de dois mecanismos, laser aleatório e espalhamento Raman estimulado, o que sugere que o material obtido também pode ser promissor para aplicações em laser aleatório Raman.

Palavras-chaves: Celulose bacteriana, fibroína da seda, nanocristais de celulose, sílica, híbridos orgânicos-inorgânicos, dispositivos fotônicos e lasers aleatórios.

LIST OF FIGURES

| | |
|--|----|
| Figure 1. Chemical structure of cellulose. Inter and intramolecular hydrogen-bonding network (adapted from (LIN; DUFRESNE, 2014a)). | 20 |
| Figure 2. a) Schematic of the unit cells for cellulose I α (triclinic, dashed line) and I β (monoclinic, solid line); b) Relative configuration of I α with respect to I β unit cell. (Adapted from (MOON et al., 2011)) | 21 |
| Figure 3. a) Transmission electron micrographs (TEM) of sugar beet CMF (adapted from ((DUFRESNE; CAVAILLE; VIGNON, 1997))); b) TEM hardwood CNF (adapted from ((SAITO et al., 2007))); c) Scanning electron micrographs (SEM) of wood CNC (adapted from ((HANLEY et al., 1997))); and BC ribbons (adapted from ((IFUKU et al., 2007))). | 22 |
| Figure 4. Hierarchical structure of cellulose; top image (from large unit to small unit): cellulose nanocrystals (CNC), micro/nanofibrillated cellulose (MFC and NFC); bottom image (from tiny unit to small unit), biosynthesis of bacterial cellulose (BC) (adapted from (LIN; DUFRESNE, 2014b)). | 23 |
| Figure 5. Schematics of idealized cellulose fibers showing one of the suggested configurations of the crystalline and amorphous regions, and cellulose nanocrystals after sulfuric acid hydrolysis of the disordered regions, exhibiting the characteristic sulfate half ester surface groups formed as a side reaction (adapted from (DOMINGUES; GOMES; REIS, 2014)). | 25 |
| Figure 6. a) Shows the formation of a chiral nematic liquid crystal phase and its coexistence with an isotropic phase in a CNC suspension of 5wt% (upper image) (GRAY, 2012). The helical arrangement of CNC is illustrated schematically next to a scanning electron microscopy image of an actual CNC helix (adapted from (GRAY, 2012)). b) Optical microscope image (crossed polars) of the bulk CNC film (scale bar 40 μm (GRAY, 2012)). c) Characteristic regularly spaced lines in an aqueous suspension with 5 wt% CNC, observed in transmission (adapted from (LAGERWALL et al., 2014)). | 27 |
| Figure 7. Selective reflection of circularly polarized light by a chiral nematic structure. The rods represent the average orientation of the director, which lies perpendicular to the films and rotates through the film (Adapted from (GIESE et al., 2015)). | 29 |
| Figure 8. a) Dry chiral nematic CNC films in a polystyrene Petri dish. Polarization optical micrograph at the center of the film. Correlation of optical and electron microscopy of the different domains; b-d) Cross-sectional SEMs images correlated with the white circles show areas b, c and d. (Adapted from (STEINER; VIGNOLINI, 2014)) | 30 |
| Figure 9. a) Evaporating and self-assembly of CNCs with silica sol-gel precursor to yield an iridescent composite, whose structural color depends on the silica loading. b) After removal of the CNCs through calcination or acid hydrolysis mesoporous sol-gel derived films are obtained that retain their intense structural colors. c) Transmittance spectra of the iridescent composite. d) Transmittance spectra of mesoporous silica films. (Adapted from (SHOPSOWITZ et al., 2010)). | 33 |
| Figure 10. Synthetic route to new nanostructured materials with chiral nematic order. In the presence of a suitable precursor, CNCs form a composite material. Removal of the template leaves a mesoporous material which can be functionalized by infiltration of the pores or used as a hard template. Alternatively, carbonization followed by removal of silica yields chiral nematic mesoporous carbon (Adapted from (GIESE et al., 2015)) | 34 |

| | |
|--|----|
| Figure 11. a) <i>Bombyx mori</i> (<i>B. mori</i>) silkworms together with two silk cocoons; b) Silk cocoons (Images from http://inhabitat.com/the-silk-pavilion-mit-researchers-to-3d-print-a-silkworm-inspired-structure/). | 36 |
| Figure 12. a) SEM images of the morphologies of silkworm cocoons from <i>Bombyx mori</i> ; (Adapted from (ZHANG et al., 2013a)) b) Structure of <i>Bombyx mori</i> silk thread (Adapted from ((PEREIRA; SILVA; DE ZEA BERMUDEZ, 2015))). | 37 |
| Figure 13. Illustration of antiparallel β -sheets, with the surface of one sheet projecting entirely methyl groups of alanine residues and the other surface of the same sheet projecting only hydrogen atoms of glycine residues. The intersheet distances alternate at 5.5\AA and 3.7\AA respectively (Adapted from (KOH et al., 2015)). | 39 |
| Figure 14. Generating new materials from silks. Native silkworm silk on the right illustration (Image from http://inhabitat.com/the-silk-pavilion-mit-researchers-to-3d-print-a-silkworm-inspired-structure/). Regenerated silk fibroin on the left illustration (Adapt from (PREDA et al., 2013)). The illustration above shows a range of materials can be generated from silks through processing into hydrogels, films fibers, sponges, microspheres, particles and tubes. The properties of these systems can be modified depending on the processing modes used and then generated into functional devices and technology platforms. | 42 |
| Figure 15. Differential Scanning Calorimetry (DSC) obtained for HOBC. | 50 |
| Figure 16. HOBC Structure, crystal-nematic transition (TC-N) and nematic-isotropic transition (TN-I) obtained by DSC. | 50 |
| Figure 17. Schematic diagram of the preparation method of the CNC/HOBC. | 52 |
| Figure 18. a and b) POM images of iridescent film of CNC showing a fingerprint texture characteristic of chiral nematic ordering; c and d) POM image of CNC/HOBC displays formation of spherulites of HOBC covering a larger area of the CNC surface. | 55 |
| Figure 19. SEM images of CNC film: a) SEM image of film surface formed by aligned nanocrystals cellulose; b) Side view of a cracked film showing the layered structure of the nanocrystals and the rod-like morphology with the rods twisted in a left-handed orientation; c) Image of fracture surface across the CNC film; d) Higher magnification side view of fracture surface across the CNC film shows the stacked layers that result from the helical pitch of the chiral nematic phase. | 56 |
| Figure 20. SEM images of CNC/ HOBC composite: a) Image of film surface of CNC covered by the liquid crystal HOBC; b) Side view of a cracked film shows the layered structure of the nanocrystals and the rod-like morphology with the rods twisting in a left-handed orientation; c) Image of cross section of fracture film (thickness $60.2\ \mu\text{m}$); d) The magnification of the side view of the fractured surface across film, shows the layered structure of the nanocrystals. | 57 |
| Figure 21. ATR-FTIR spectra: a) HOBC, b) CNC and c) CNC/HOBC. | 58 |
| Figure 22. Emission spectra of neat HOBC and CNC/HOBC composite recorded at 298K, under excitation at 280nm. | 59 |
| Figure 23. Transmission spectra of the films CNC and CNC/ HOBC | 60 |
| Figure 24. a) Specular reflectance of CNC/HOBC composite between 20 and 70 degree; b) Variation of the peak position of the reflectance spectra as function of the $\cos \theta$ for CNC/HOBC. | 61 |
| Figure 25. Transmission spectra as function of the temperature: a) HOBC; b) CNC/HOBC. | 62 |
| Figure 26. TOM micrographs of CNC/HOBC during heating taken at: (a) $30\text{ }^\circ\text{C}$ (b) $47\text{ }^\circ\text{C}$, (c) $56\text{ }^\circ\text{C}$, (d) $60\text{ }^\circ\text{C}$ and during cooling at: (e) $60\text{ }^\circ\text{C}$ (f) $55\text{ }^\circ\text{C}$ (g) $45\text{ }^\circ\text{C}$ (h) $30\text{ }^\circ\text{C}$. (scale bar, $200\ \mu\text{m}$). | 63 |

| | |
|---|----|
| Figure 27. TM-AFM ($3\mu\text{m} \times 3\mu\text{m}$) height (a) and phase (b) images of CNC and TM-AFM height (a) and phase (b) images of CNC/HOBC film. | 64 |
| Figure 28. a) AFM phase image ($3\mu\text{m} \times 3\mu\text{m}$) and EFM phase images ($3\mu\text{m} \times 3\mu\text{m}$) of CNC/HOBC film obtained applying b) 0 V, c) 6 V and d) -6 V. | 65 |
| Figure 29. Photograph of CNC/silica composites films with different amount of silica. Viewing is normal to the film surface. | 70 |
| Figure 30. Photograph of CNC/silica doped with Rh6G composites films with different amount of silica. Viewing is normal to the film surface. | 71 |
| Figure 31. Specular reflectance scheme. | 72 |
| Figure 32. The modular experimental setup to measurements of photoluminescence spectra as function of the angle ($-90^\circ < \theta < 90^\circ$). | 73 |
| Figure 33. TG curves of composite films) CNC-Rh; b) CS1-Rh; c) CS2-Rh; d) CS3-CS4-Rh. | 74 |
| Figure 34. Polarized optical microscopy (POM) images with crossed polarizers: a) CS1-Rh and b) CS4-Rh. | 75 |
| Figure 35. a) Photograph of composite CS4-Rh; b) oblique sectional view of a fracture surface across of composite CS4-Rh; c) and d) SEM images of its cross –section of CS4-Rh. | 76 |
| Figure 36. a) Transmission spectra of CNC, CS1, CS2, CS3 and CS4; b) Variation of the peak position of the reflectance spectra as function of the $\cos \theta$ for CNC/silica composites. . | 77 |
| Figure 37. a) Transmission spectra of CNC, CS1-Rh, CS2-Rh, CS3-Rh and CS4-Rh; b) Variation of the peak position of the reflectance spectra as function of the $\cos \theta$ for CNC/silica composites doped with Rh6G. | 77 |
| Figure 38. Figure S3. a) Specular reflectance of CS4 between 20 and 60 degree, b) Specular reflectance of CS4-Rh between 15 and 60 degree. | 78 |
| Figure 39. Variation of the P of chiral nematic structure of composites with different silica proportion. | 80 |
| Figure 40. Emission spectra of composite CNC/silica doped with Rh6G in front face acquisition mode excited at 348nm. | 81 |
| Figure 41. Emission spectra of CNC film in front face acquisition mode excited at 345nm. . | 82 |
| Figure 42. a) Emission spectra of CS4-Rh composite as function of the detection angle (0° to -90°), excited at 348nm; b) Emission spectra of CS4-Rh composite as function of the detection angle (0° to 90°), excited at 348nm; c) Variation of the λ_0 and linewidth of emission bands of composite CS4-Rh as function of the detection angle ($-90^\circ < \theta < 90^\circ$); d) Variation of the maximum wavelength (λ_0) of emission bands of composite BC-Rh as function of the detection angle ($-90^\circ < \theta < 90^\circ$). | 84 |
| Figure 43. a) Color diagram of reflection of CS4-Rh composite film as function of the detection angle ($0^\circ < \theta < 60^\circ$); b) Color diagram of emission color of CS4-Rh composite film as function of the detection angle ($0^\circ < \theta < 90^\circ$), excited at 348nm | 85 |
| Figure 44. Emission spectra of CS4-Rh excited at 348 nm acquired at 20° and 90° . Reflectance spectra acquired at 20° and 50° | 85 |
| Figure 45. Variation of the maximum emission wavelength for composite films CNC/silica doped with Rh6G as function of the detection angle ($-90^\circ < \theta < 90^\circ$) a) CNC-Rh; b) CS1-Rh; c) CS2-Rh; d) CS3-Rh. | 85 |
| Figure 46. a) Photograph of silica/fibroin hybrids monoliths. b) SEM image of the surface of monolith SF3; c) SEM image of agglomerate of fibroin nanofibers on the surface of monolith SF3; d) Image of the fracture of the monolith SF3. | 87 |

| | |
|--|-----|
| Figure 47. Thermogravimetric curves of silica/fibroin hybrid monoliths: a) SF0; b) SF1; c) SF2; d) SF3 and e) SF4. | 98 |
| Figure 48. Raman spectra of silica/fibroin hybrid monoliths: a) SF1; b) SF2; c) SF3 and d) SF4..... | 100 |
| Figure 49. $^{29}\text{Si}\{^1\text{H}\}$ CP MAS spectra of silica/fibroin hybrid monoliths contained differents fibroin concentrations: a) SF1; b) SF3 and d) SF4. | 101 |
| Figure 50. $^{13}\text{C}\{^1\text{H}\}$ CP-MAS spectra of silica/fibroin hybrid monoliths containing differents fibroin concentrations: a) SF1; b) SF3 and c) SF4. | 102 |
| Figure 51. ^1H spin echo MAS spectrum of SF4 silica/fibroin hybrid monoliths. | 103 |
| Figure 52. FSLG $^{13}\text{C}\{^1\text{H}\}$ CP HETCOR spectra of SF4 sample obtained with two contact times 0.5 e 2.5ms. ($\nu_r=14\text{kHz}$, $\nu_0=188.6\text{MHz}$, $t_1=5\text{s}$). | 105 |
| Figure 53. A schematic illustration of the self-assembly of fibroin nanofibers inside the bulk of silica composites materials and posterior calcination of fibroin nanofibers to form porous ceramic..... | 106 |
| Figure 54. a) Photograph of silica monoliths; b) SEM image of the porous surface of monolith S3; c and d) Images of fracture of S3, showing porous with diameter of hundreds of nanometers inside the bulk of silica. | 107 |
| Figure 55. a) Nitrogen adsorption/desorption isotherms; b) Pore size distribution; c) plot of $\log(\ln(\rho))$ versus $\log(\theta)$; d) Evolution of the specific surface area, pore diameter and surface fractal dimension of the samples. | 108 |
| Figure 56. a) Peak intensity vs. pumping energy per pulse showing the nonlinear behavior of porous silica monoliths containing Rh6G; b) Full width half maximum (FWHM) linewidth vs. pumping energy per pulse. The minimum linewidth was ≈ 4 nm for pumping above the threshold. | 111 |
| Figure 57. Spectral behavior of the S4 containing Rh6G as of pumping energy per pulse. Minimum linewidth observed is about 0.5 nm. The inset shows the yellow emission colour of the sample S4 doped with Rh6G excited with irradiated with a laser at 532nm. | 112 |

LIST OF TABLES

| | |
|---|-----|
| Table 1. Examples of CNCs isolated from different sources..... | 26 |
| Table 2. Variation of the helicoidal pitch of composites films..... | 79 |
| Table 3. Decay time values ($\lambda_{\text{EXC}}= 330\text{nm}$): CNC ($\lambda_{\text{EM}}= 480\text{nm}$) (τ_1); Dye-doped CNC/silica composites, $\lambda_{\text{EM}}= 400\text{nm}$ (τ_1) and $\lambda_{\text{EM}}= 560 \text{ nm}$ (τ_2). Quantum yield values: CNC-Rh, $\lambda_{\text{EXC}}= 528\text{nm}$ and $\lambda_{\text{EM}}= 567\text{nm}$; Dye-doped CNC/silica composites, $\lambda_{\text{EXC}}= 528\text{nm}$ and $\lambda_{\text{EM}}= 556\text{nm}$ | 83 |
| Table 4. Heat ramp used to calcinate the fibroin fraction in the silica/fibroin hybrids monoliths. Heat temperature, heating rate and the time that the samples were kept in the matching temperature are presented. | 94 |
| Table 5. Samples composition and degradation temperature of fibroína (Tonset) determined by thermogravimetric curves. | 99 |
| Table 6. Physico-chemical properties of calcinated samples..... | 109 |
| Tabela 7. Values of energy thresholds and slope efficiency of silica monoliths..... | 111 |

LIST OF ABBREVIATIONS

AFM- Atomic Force Microscopy
8CB - 4-Cyano-4'octylbiphenyl
BC - Bacterial cellulose
BET- Brunauer, Emmett, Teller
CNC - Cellulose nanocrystal
DP- Degree of polymerization
DSC- Differential scanning calorimetry
EFM - Electrostatic force microscopy
EPE- Excitation pulse energy
HOBC- 4'-(hexyloxy)-4-biphenyl carbonitrile
IOH- Inorganic organic hybrids
LCs - Liquid crystals
MFC - Microfibrillated cellulose
NFC - Nanofibrillated cellulose
 M_w - Molecular weight
NMR - Nuclear magnetic resonance spectroscopy
PLA - Poly(l-lactic acid)
PL- Photoluminescence
POM- Polarized optical microscopy
RL- Random laser
Rh6G- Rhodamine 6G
SF- Silk Fibroin
SEM - Scanning electron microscopy
TOM - Transmission optical microscopy
TEOS - Tetraethylorthosilicate
TEM - Transmission electron microscopy
TG- Thermogravimetric
UV - Ultraviolet

CONTENTS

| | |
|---|----|
| 1. INTRODUCTION | 19 |
| 1.1. Cellulose | 19 |
| 1.1.1. Nanocelluloses. | 21 |
| 1.1.2. Cellulose nanocrystals..... | 24 |
| 1.1.3 Self-assembly and organization of cellulose nanocrystals. | 26 |
| 1.1.4. Cellulose nanocrystals as templates for the chemical synthesis of inorganic materials..... | 32 |
| 1.2. Silk fibroin | 35 |
| 1.2.1 Primary Structure of silk fibroin. | 37 |
| 1.2.2. Secondary structure of silk fibroin..... | 38 |
| 1.2.3. Extraction and processing of silk fibroin. | 40 |
| 2. OBJECTIVES | 45 |
| PART I. MULTIFUNCTIONAL MATERIALS BASED ON CELLULOSE NANOCRYSTALS. | 46 |
| 3. Optical platform based on cellulose nanocrystals (CNC) – 4-(hexyloxy)-4-biphenylcarbonitrile (HOBC) bi-phase nematic liquid crystal films | 47 |
| 3.1. Introduction. | 47 |
| 3.2. Materials and methods. | 49 |
| 3.2.1. Materials..... | 49 |
| 3.2.2. Preparation of cellulose nanocrystals (CNC). | 51 |
| 3.2.3. Preparation of the composite film. | 52 |
| 3.2.4. Characterization of CNC and CNC/HOBC films..... | 52 |
| 3.3 Results and discussions | 54 |
| 3.3.1- Morphological Characterization. | 54 |
| 3.3.2- Structural Characterization. | 57 |
| 3.3.3- Optical Characterization. | 59 |
| 3.4. Conclusions | 66 |
| 4. Cellulose based photonic materials displaying modulated photoluminescence | 67 |
| 4.1. Introduction | 67 |
| 4.2. Materials and methods. | 69 |
| 4.2.1-Preparation of bacterial cellulose membranes: | 69 |
| 4.2.2-Preparation of cellulose nanocrystals (CNC):..... | 69 |
| 4.2.3-Preparation of nanocrystalline CNC-silica composite films. | 70 |
| 4.2.4- Preparation of nanocrystalline CNC-silica composite doped with broad band emitters (Rhodamine 6G (Rh6G)):..... | 71 |

| | |
|--|------------|
| 4.2.5. Characterization of CNC and composite films..... | 71 |
| 4.2- Results and discussions..... | 73 |
| 4.4 Conclusions | 87 |
| PART II. MULTIFUNCTIONAL MATERIALS USING SILK FIBROIN AS A BIOTEMPLATE. | 89 |
| 5. Silk fibroin as a biotemplate for hierarchical porous silica monoliths for random laser applications | 90 |
| 5.1. Introduction | 90 |
| 5.2. Materials and methods. | 92 |
| 5.2.1- Extraction of silk fibroin..... | 92 |
| 5.2.2-Preparation of organic-inorganic hybrids monoliths based on silica and fibroin. | 93 |
| 5.2.2-Preparation of porous silica monoliths..... | 93 |
| 5.2.3-Preparation of porous monoliths of silica containing Rh6G. | 94 |
| 5.2.4-Characterization of materials. | 94 |
| 5.3. Results and discussions | 95 |
| 5.3.1. Characterization of organic-inorganic hybrid monoliths based on silica and fibroin. | 96 |
| 5.3.2. Characterization of porous silica monoliths..... | 107 |
| 5.3.3. Characterization of the random laser action in the silica monoliths containing Rh6g. | 110 |
| 5.3. Conclusions | 113 |
| 6. GENERAL CONCLUSION. | 114 |
| REFERENCES | 148 |

Organization of the thesis

In light of recent studies, cellulose nanocrystals extracted from bacterial cellulose and regenerated silk fibroin from silkworm cocoons are attractive alternatives to design multifunctional materials, reason why this is the focus of such thesis.

Therefore, this study is divided into four chapters. The first chapter is devoted to introduce cellulose nanocrystals and silk fibroins, their preparation, properties and recent applications. Subsequently to the introductory section, the preparation of multifunctional materials based on cellulose nanocrystal is presented on second and third chapter.

Further, the second chapter presents the preparation of free-standing CNC films coated with low molecular weight nematic liquid crystal (LC), 4'-(hexyloxy)-4-biphenylcarbonitrile (HOBC), which integrate iridescence, conductive and thermal response. Such composite films were morphologically characterized by the SEM and POM, and optically by electron spectroscopy. Emphasis is given to the characterization of morphological and optical properties of the composite in function of the temperature. Additionally, the conductive response brush surface was evaluated using electrostatic force microscopy (EFM) measurements.

Afterwards, the third chapter encompasses the preparation and characterization of iridescent luminescent films based on dye-doped CNC/silica composites. Such composite films were morphologically characterized through SEM and POM, and optically by electron spectroscopy. In this section, the focus is given to the investigation of the influence of photonic structure of films on light emission from dye-doped CNC/HOBC composites, using luminescence spectroscopy measurements in function of the detection angle.

Finally, in the last chapter, the synthesis of organic inorganic hybrids monoliths based on silica and silk fibroin is described. The hybrids monoliths were morphologically characterized by SEM and structural characterized by Raman, and solid state RMN spectroscopies. Additionally, the chapter also describes the preparation of porous silica monoliths using the fibroin nanofibers as a biotemplate. The silica monoliths were morphologically characterized by SEM and their porous structure were characterized via nitrogen adsorption experiments. Moreover, the random laser action of silica monoliths was investigated.

1. INTRODUCTION

Commonly, natural materials provide a convincing template to reinterpretation and, in some cases, simplification of modern manufacturing, while rendering them sustainability and green. Biopolymers, produced and modified by living organisms are the pillars of self-assembly on structurally hierarchical micro and nanoscale systems, which occur naturally, such as chitin of butterfly wings, beetles exoskeletons, keratin in peacock feathers (PENNISI, 2013; WEAVER et al., 2012; YANG et al., 2013), and so forth. From the material science perspective, biopolymers can be a versatile source to design structured inorganic or inorganic/organic materials in the laboratory. The interest in the direct use and re-engineering of natural polymers as platforms for the development of technology materials has been growing in recent years. The challenge using these materials is to identify, among the options available, materials that present adequate properties to interface with current technology. In addition, such materials should be widely available and have competitive costs in the world market. Thus, in this thesis, there is an interest in the opportunities offered by bacterial cellulose produced through the *Gluconacetobacter xylinus* bacteria and silk fibroin extracted from *Bombyx mori* silkworm cocoons biopolymers as platforms for technological applications.

6. GENERAL CONCLUSION.

The main goal of this PhD research was to exploit the self-assembly properties of cellulose nanocrystals (CNC) extracted from bacterial cellulose produced by *Acetobacter xylinum* bacteria, as well as, regenerated silk fibroin (SF) stemmed from the cocoons of the silkworm (*Bombyx mori*) in order to prepare nanostructured materials for optical applications. In this context, different multifunctional materials were prepared.

Initially, a composite structure formed from two different liquid crystal forming materials, a low molecular weight 4'-(hexyloxy)-4-biphenylcarbonitrile (HOBC) and cellulose nanocrystals (CNC), was prepared. The HOBC was applied on a CNC film by simple painting. In this case, HOBC liquid crystal was used as a functional compound to promote new properties of the CNC films. The new material here proposed was obtained as a free-standing iridescent film, with chiral nematic structure. The films exhibited modulated optical properties, in response to thermal gradient or relatively small electrical voltage, in addition to liquid crystal properties of the CNC films. Further, the HOBC coating did not change the morphological and optical properties of the cellulose nanocrystal film. It is noteworthy that, for this record, cellulose nanocrystals iridescent films with thermochromic or conductive properties have not been reported in the literature yet. This work presented a new platform for utilization of CNC film, which opens the possibility of applications for this material in the field of thermo- and electro optical devices.

Moreover, still in the field of optical applications of CNC, the preparation of iridescent luminescent composite films by combining tetraethoxysilane (TEOS) to a CNC suspension and to ethanolic solutions of a broad band emitter (Rhodamine 6G (Rh6G)) was demonstrated. The composites were obtained as free-standing films with chiral nematic organization. The morphological and optical characterization demonstrated that the insertion of silica in the composites implies in the control of optical film properties, as well as in the improvement in the quality of the photoluminescence material. The cellulose based photonic materials also displayed modulated photoluminescence with detecting angle. This behavior suggests that the photonic structure with chiral nematic ordering has a strong effect in the emission spectra. In addition, it was demonstrated that this effect is tuned with the stop band position of composite films. Taken the advantages of the luminescence and chiral nematic ordering integration of the CNC films, some examples have been reported in the literature. However, in all of them, their focus was given to the modulating spontaneous emission through circularly polarized excitation of the samples. In this thesis, it is suggested a novel strategy to modulate the emission of

luminescent species exploring the inner filter effect of the periodic structure of films. Thus, it holds that this multifunctional material can be attractive to develop new optical devices with potential for various applications, such as, sensors, lasers or tunable filters.

Finally, multifunctional organic inorganic hybrids based on silica and silk fibroin were developed. Although there are several reports on the literature that present design silica/fibroin hybrids materials, this was the first time the preparation of robust monoliths containing until 15.8 wt% of fibroin was demonstrated. In addition, it was exhibited that these unique materials are formed by 3D network silica gel reinforced by the interpenetrated fibroin nanofibers with preferential crystalline β -sheet conformation, which can lead to an improve of the robustness and the hardness of monoliths when compared with silica xerogel. Likewise, considering the biocompatible property of these materials, the combination of silica and silk leads to very promising and versatile materials with foreseen application in a variety of domains, including bone regeneration. However, it was also possible to demonstrate that the fibroin nanofibers can be used as biotemplates, acting as a sacrificial material to develop porous silica monoliths. These porous monoliths demonstrated efficient RL action, operating in a diffusive regime in hierarchical macro–mesoporous network. In addition, when higher values of EPE are inserted, the emission spectra obtained present the stimulated emission and stimulated Raman scattering mechanisms coupled. These results suggest that designed materials can be promising for new applications of the RL phenomenon, such as specklefree laser imaging and random Raman laser.

REFERENCES

- ABEER, M. M. et al. A review of bacterial cellulose-based drug delivery systems: their biochemistry, current approaches and future prospects. **Journal of Pharmacy and Pharmacology**, v. 66, n. 8, p. 1047-1061, 2014.
- ABITBOL, T. et al. Nanocellulose, a tiny fiber with huge applications. **Current Opinion in Biotechnology**, v. 39, p. 76-88, 2016.
- ALTMAN, G. H. et al. Silk-based biomaterials. **Biomaterials**, v. 24, n. 3, p. 401-416, 2003.
- ANEDDA, A. et al. Rhodamine 6G-SiO₂ hybrids: a photoluminescence study. **Journal of Non-Crystalline Solids**, v. 351, n. 21/23, p. 1850-1854, 2005.
- ANEDDA, A. et al. Formation of fluorescent aggregates in rhodamine 6G doped silica glasses. **Journal of Non-Crystalline Solids**, v. 353, n. 5/7, p. 481-485, 2007.
- APPLEGATE, M. B. et al. Biocompatible silk step-index optical waveguides. **Biomedical Optics Express**, v. 6, n. 11, p. 4221-4227, 2015.
- ARAKI, J.; KUGA, S. Effect of trace electrolyte on liquid crystal type of cellulose microcrystals. **Langmuir**, v. 17, n. 15, p. 4493-4496, 2001.
- ARAKI, J. et al. Flow properties of microcrystalline cellulose suspension prepared by acid treatment of native cellulose. **Colloids and Surfaces A: Physicochemical and Engineering Aspects**, v. 142, n. 1, p. 75-82, 1998.
- ARAKI, J. et al. Influence of surface charge on viscosity behavior of cellulose microcrystal suspension. **Journal of Wood Science**, v. 45, n. 3, p. 258-261, 1999.
- ARCOS, D.; VALLET-REGÍ, M. Sol-gel silica-based biomaterials and bone tissue regeneration. **Acta Biomaterialia**, v. 6, n. 8, p. 2874-2888, 2010.
- ARRIGHI, V. et al. Fine Structure and optical properties of cholesteric films prepared from cellulose 4-methylphenyl urethane/n-vinyl pyrrolidinone solutions. **Macromolecules**, v. 35, n. 19, p. 7354-7360, 2002.
- ASAKURA, T. et al. Heterogeneous structure of silk fibers from *Bombyx mori* resolved by C-13 solid-state NMR spectroscopy. **Journal of the American Chemical Society**, v. 124, n. 30, p. 8794-8795, 2002.
- ASAKURA, T. et al. Evidence from ¹³C solid-state NMR spectroscopy for a lamella structure in an alanine-glycine copolypeptide: a model for the crystalline domain of *Bombyx mori* silk fiber. **Protein Science**, v. 14, n. 10, p. 2654-2657, 2005.
- ASAKURA, T. et al. Elucidating silk structure using solid-state NMR. **Soft Matter**, v. 9, n. 48, p. 11440-11450, 2013.
- BACHELARD, N. et al. Disorder as a playground for the coexistence of optical nonlinear. **ACS Photonics**, v. 1, n. 11, p. 1206-1211, 2014.

- BALACHANDRAN, R. M.; LAWANDY, N. M. Laser action in strongly scattering media. In: INTERNATIONAL QUANTUM ELECTRONICS CONFERENCE, 21st, 1994, Anaheim. **Proceedings...** Washington, DC: Optical Society of America, 1994, p. QFE1.
- BARUD, H. S. et al. Bacterial cellulose-silica organic-inorganic hybrids. **Journal of Sol-Gel Science and Technology**, v. 46, n. 3, p. 363-367, 2008.
- BARUD, H. S. et al. Antimicrobial bacterial cellulose-silver nanoparticles composite membranes. **Journal of Nanomaterials**, v. 2011, 2011. doi:10.1155/2011/721631.
- BATISTA, J. N. M. et al. Controlling silicate meso-structures using sucupira oil as a new swelling agent. **Applied Surface Science**, v. 258, n. 12, p. 5111-5116, 2012.
- BAUDOQUIN, Q. et al. A cold-atom random laser. **Nature Physics**, v. 9, n. 6, p. 357-360, 2013.
- BECK, S.; BOUCHARD, J.; BERRY, R. Controlling the reflection wavelength of iridescent solid films of nanocrystalline cellulose. **Biomacromolecules**, v. 12, n. 1, p. 167-172, 2011.
- BECK, S. et al. Controlled production of patterns in iridescent solid films of cellulose nanocrystals. **Cellulose**, v. 20, n. 3, p. 1401-1411, 2013.
- BECK-CANDANEDO, S.; ROMAN, M.; GRAY, D. G. Effect of reaction conditions on the properties and behavior of wood cellulose nanocrystal suspensions. **Biomacromolecules**, v. 6, n. 2, p. 1048-1054, 2005.
- BETTINGER, C. J. et al. Silk fibroin microfluidic devices. **Advance Materials**, v. 19, n. 5, p. 2847-2850, 2007.
- BRITO-SILVA, A. M. et al. Random laser action in dye solutions containing Stöber silica nanoparticles. **Journal of Applied Physics**, v. 108, n. 3, p. 33508/1- 33508/2, 2010.
- BROER, D. J.; LUB, J.; MOL, G. N. Wide-band reflective polarizers from cholesteric polymer networks with a pitch gradient. **Nature**, v. 378, p. 467-469, 1995.
- BROWN, R. M. Cellulose structure and biosynthesis: what is in store for the 21st century? **Journal of Polymer Science Part A: Polymer Chemistry**, v. 42, n. 3, p. 487-495, 2004.
- BROWN, S. P.; SPIESS, H. W. Advanced solid-state NMR methods for the elucidation of structure and dynamics of molecular, macromolecular and supramolecular systems. **Chemical Reviews**, v. 101, p. 4125-4155, 2001.
- BUJDÁK, J. Effect of the layer charge of clay minerals on optical properties of organic dyes. A review. **Applied Clay Science**, v. 34, n. 1/4, p. 58-73, 2006.
- CAMPBELL, M. G.; TASINKEVYCH, M.; SMALYUKH, I. I. Topological polymer dispersed liquid crystals with bulk nematic defect lines pinned to handlebody surfaces. **Physical Review Letters**, v. 112, n. 19, p. 19780/1-19780/5, 2014.

CAO, H. et al. Random laser action in semiconductor powder. **Physical Review Letters**, v. 82, n. 11, p. 2278-2281, 1999.

CAPADONA, J. R. et al. Polymer nanocomposites with nanowhiskers isolated from microcrystalline cellulose. **Biomacromolecules**, v. 10, n. 4, p. 712-716, 2009.

CARBONARO, C. M. et al. Light assisted dimer to monomer transformation in heavily doped rhodamine 6G-porous silica hybrids. **Journal of Physical Chemistry B**, v. 113, n. 15, p. 5111-5116, 2009.

CARREÑO, S. J. M. et al. Interplay between random laser performance and self-frequency conversions in $\text{Nd}_x\text{Y}_{1.00-x}\text{Al}_3(\text{BO}_3)_4$ nanocrystals powders. **Optical Materials**, v. 54, p. 262-268, 2016.

CHAO, P. G. et al. Silk hydrogel for cartilage tissue engineering. **Journal of Biomedical Materials Research Part B: Applied Biomaterials**, v. 95, n. 1, p. 84-90, 2010.

CHOI, S. S. et al. Electrically tuneable liquid crystal photonic bandgaps. **Advanced Materials**, v. 21, n. 38/39, p. 3915-3918, 2009.

CHU, G. et al. Chiral nematic mesoporous films of $\text{Y}_2\text{O}_3:\text{Eu}^{3+}$ with tunable optical properties and modulated photoluminescence. **Journal of Materials Chemistry C**, v. 2, p. 9189-9195, 2014.

CHU, G. et al. Chiral electronic transitions of $\text{YVO}_4:\text{Eu}^{3+}$ nanoparticles in cellulose based photonic materials with circularly polarized excitation. **Journal of Materials Chemistry C**, v. 3, n. 14, p. 3384-3390, 2015a.

CHU, G. et al. Optically tunable chiral plasmonic guest-host cellulose films weaved with long-range ordered silver nanowires. **ACS Applied Materials and Interfaces**, v. 7, n. 22, p. 11863-11870, 2015b.

COASNE, B. Multiscale adsorption and transport in hierarchical porous materials. **New Journal of Chemistry**, v. 40, n. 5, p. 4078-4094, 2016.

COLES, H. J.; PIVNENKO, M. N. Liquid crystal 'blue phases' with a wide temperature range. **Nature**, v. 436, n. 7053, p. 997-1000, 2005.

DANG, Q. et al. Silk fibroin/montmorillonite nanocomposites: effect of pH on the conformational transition and clay dispersion. **Biomacromolecules**, v. 11, n. 7, p. 1796-1801, 2010.

DARDER, M.; ARANDA, P.; RUIZ-HITZKY, E. Bionanocomposites: a new concept of ecological, bioinspired, and functional hybrid materials. **Advanced Materials**, v. 19, n. 10, p. 1309-1319, 2007.

DE VRIES, H. Rotatory power and other optical properties of certain liquid crystals. **Acta Crystallographica**, v. 4, n. 3, p. 219-226, 1951.

DEBZI, H. M.; CHANZY, H. The $I\alpha \rightarrow I\beta$ transformation of highly crystalline cellulose by annealing in various mediums. **Macromolecules**, v. 24, n. 26, p. 6816-6822, 1991.

DOANE, J. W. et al. Field controlled light scattering from nematic microdroplets. **Applied Physics Letters**, v. 48, n. 4, p. 269-271, 1986.

DOMINGUES, R. M. A.; GOMES, M. E.; REIS, R. L. The potential of cellulose nanocrystals in tissue engineering strategies. **Biomacromolecules**, v. 15, n. 7, p. 2327-2346, 2014.

DONG, X. M.; REVOL, J.-F.; GRAY, D. G. Effect of microcrystallite preparation conditions on the formation of colloid crystals of cellulose. **Water**, v. 5, p. 19-32, 1998.

DRIESEN, K. et al. Near-infrared luminescence emitted by an electrically switched liquid crystal cell. **Journal of Luminescence**, v. 127, n. 2, p. 611-615, 2007.

DRZAIC, P. S. Polymer dispersed nematic liquid crystal for large area displays and light valves. **Journal of Applied Physics**, v. 60, n. 6, p. 2142-2148, 1986.

DUFRESNE, A.; CAVAILLE, J.-Y.; VIGNON, M. R. Mechanical behavior of sheets prepared from sugar beet cellulose microfibrils. **Journal of Applied Polymer Science**, v. 64, n. 6, p. 1185-1194, 1997.

DUJARDIN, E.; BLASEBY, M.; MANN, S. Synthesis of mesoporous silica by sol-gel mineralisation of cellulose nanorod nematic suspensions. **Journal of Materials Chemistry**, v. 13, n. 4, p. 696-699, 2003.

DUNDERDALE, G. J. et al. Large-scale and environmentally friendly synthesis of pH-responsive oil-repellent polymer brush surfaces under ambient conditions. **ACS Applied Materials and Interfaces**, v. 6, p. 11864-11868, 2014.

EICHHORN, S. J. Cellulose nanowhiskers: promising materials for advanced applications. **Soft Matter**, v. 7, n. 2, p. 303-315, 2011.

ELAZZOUZI-HAFRAOUI, S. et al. The shape and size distribution of crystalline nanoparticles prepared by acid hydrolysis of native cellulose. **Biomacromolecules**, v. 9, n. 1, p. 57-65, 2007.

FAVIER, V.; CHANZY, H.; CAVAILLE, J. Y. Polymer nanocomposites reinforced by cellulose whiskers. **Macromolecules**, v. 28, p. 6365-6367, 1995.

FREDDI, G. et al. Silk fibroin/cellulose blend films: preparation, structure, and physical properties. **Journal of Applied Polymer Science**, v. 56, n. 12, p. 1537-1545, 1995.

FU, L.; ZHANG, J.; YANG, G. Present status and applications of bacterial cellulose-based materials for skin tissue repair. **Carbohydrate Polymers**, v. 92, n. 2, p. 1432-1442, 2013.

GAGNÉ, M.; KASHYAP, R. Demonstration of a 3 mW threshold Er-doped random fiber laser based on a unique fiber Bragg grating. **Optics Express**, v. 17, n. 21, p. 19067-19074, 2009.

GAIKWAD, P. et al. Competition and coexistence of Raman and random lasing in silica/titania-based solid foams. **Advanced Optical Materials**, v. 3, n. 11, p. 1640-1651, 2015.

GALARNEAU, A. et al. Comptes rendus chimie hierarchical porous silica monoliths: a novel class of microreactors for process intensification in catalysis and adsorption. **Comptes Rendus Chimie**, v. 19, n. 1/2, p. 231-247, 2016.

GANESAN, L. M. et al. Piezo-optical and electro-optical behaviour of nematic liquid crystals dispersed in a ferroelectric copolymer matrix. **Journal of Physics D: Applied Physics**, v. 43, n. 1, p. 015401/1-015401/6, 2010.

GARCIA DE RODRIGUEZ, N. L. G.; THIELEMANS, W.; DUFRESNE, A. Sisal cellulose whiskers reinforced polyvinyl acetate nanocomposites. **Cellulose**, v. 13, n. 3, p. 261-270, 2006.

GARCÍA-REVILLA, S. et al. Ultrafast random laser emission in a dye-doped silica gel powder. **Optics Express**, v. 16, n. 16, p. 12251-12263, 2008.

GARCÍA-REVILLA, S. et al. Low threshold random lasing in dye-doped silica nano powders. **Optics Express**, v. 17, n. 15, p. 13202-13215, 2009.

GEBAUER, D. et al. A transparent hybrid of nanocrystalline cellulose and amorphous calcium carbonate nanoparticles. **Nanoscale**, v. 3, n. 9, p. 3563-3566, 2011.

GIESE, M. et al. Thermal switching of the reflection in chiral nematic mesoporous organosilica films infiltrated with liquid crystals. **ACS Applied Materials and Interfaces**, v. 5, p. 6854-6859, 2013.

GIESE, M. et al. Functional materials from cellulose-derived liquid-crystal templates. **Angewandte Chemie International Edition**, v. 54, n. 10, p. 2888-2910, 2015.

GRAY, D. G. SEM imaging of chiral nematic films cast from cellulose nanocrystal suspensions. **Cellulose**, v. 19, n. 5, p. 1599-1605, 2012.

GRUNERT, M.; WINTER, W. T. Nanocomposites of cellulose acetate butyrate reinforced with cellulose nanocrystals. **Journal of Polymers and the Environment**, v. 10, n. 1/2, p. 27-30, 2002.

GUIOCHON, G. Monolithic columns in high-performance liquid chromatography. **Journal of Chromatography A**, v. 1168, n. 1/2, p. 101-168, 2007.

GUTIERREZ, J. et al. Conductive properties of TiO₂ / bacterial cellulose hybrid fibres. **Journal of Colloid And Interface Science**, v. 377, n. 1, p. 88-93, 2012.

HABIBI, Y. Key advances in the chemical modification of nanocelluloses. **Chemical Society Reviews**, v. 43, n. 5, p. 1519-1542, 2014.

HABIBI, Y.; LUCIA, L. A. Nanocelluloses: emerging building blocks for renewable materials. In: _____. (Ed). **Polysaccharide building blocks: sustainable approach to the development of renewable biomaterials**. Hoboken: Wiley, 2012. Chap. 3 p. 105-125.

HABIBI, Y.; LUCIA, L. A.; ROJAS, O. J. Cellulose nanocrystals: chemistry, self-assembly, and applications. **Chemical Reviews**, v. 110, p. 3479-3500, 2010.

HABIBI, Y. et al. Bionanocomposites based on poly (ϵ -caprolactone) -grafted cellulose nanocrystals by ring-opening polymerization. **Journal of Materials Chemistry**, v. 18, n. 41, p. 5002-5010, 2008.

HANLEY, S. J. et al. Atomic force microscopy and transmission electron microscopy of cellulose from *Micrasterias denticulata*; evidence for a chiral helical microfibril twist. **Cellulose**, v. 4, n. 3, p. 209-220, 1997.

HE, S.-J.; VALLUZZI, R.; GIDO, S. P. Silk I structure in *Bombyx mori* silk foams. **International Journal of Biological Macromolecules**, v. 24, n. 2, p. 187-195, 1999.

HIRAI, A. et al. Phase separation behavior in aqueous suspensions of bacterial cellulose nanocrystals prepared by sulfuric acid treatment. **Langmuir**, v. 25, n. 1, p. 497-502, 2008.

HOKR, B. H. et al. Bright emission from a random Raman laser. **Nature Communications**, v. 5, 2014. doi:10.1038/ncomms5356.

HOPKINS, A. M. et al. Silk hydrogels as soft substrates for neural tissue engineering. **Advanced Functional Materials**, v. 23, n. 41, p. 5140-5149, 2013.

HOSSAIN, K. S. et al. Dilute-solution properties of regenerated silk fibroin. **The Journal of Physical Chemistry B**, v. 107, p. 8066-8073, 2003.

HOU, A.; CHEN, H. Preparation and characterization of silk/silica hybrid biomaterials by sol-gel crosslinking process. **Materials Science and Engineering B: Solid-State Materials for Advanced Technology**, v. 167, n. 2, p. 124-128, 2010.

HU, K. et al. Preparation of fibroin/recombinant human-like collagen scaffold to promote fibroblasts compatibility. **Journal of Biomedical Materials Research Part A**, v. 84, n. 2, p. 483-490, 2008.

HU, W. et al. Functionalized bacterial cellulose derivatives and nanocomposites. **Carbohydrate Polymers**, v. 101, p. 1043-1060, 2014.

HU, X. et al. Regulation of silk material structure by temperature-controlled water vapor annealing. **Biomacromolecules**, v. 12, n. 5, p. 1686-1696, 2011.

HUANG, L. et al. Single-strand spider silk templating for the formation of hierarchically ordered hollow mesoporous silica fibers. **Journal of Materials Chemistry**, v. 13, n. 4, p. 666-668, 2003.

HUANG, Y. et al. Recent advances in bacterial cellulose. **Cellulose**, v. 21, n. 1, p. 1-30, 2014.

IFUKU, S. et al. Surface modification of bacterial cellulose nanofibers for property enhancement of optically transparent composites: dependence on acetyl-group DS. **Biomacromolecules**, v. 8, n. 6, p. 1973-1978, 2007.

IGNESTI, E. et al. Experimental and theoretical investigation of statistical regimes in random laser emission. **Physical Review A**, v. 88, n. 3, p. 33820/1-33820/8, 2013.

INOUE, S. et al. Silk fibroin of *Bombyx mori* is secreted, assembling a high molecular mass elementary unit consisting of H-chain, L-chain, and P25, with a 6: 6: 1 molar ratio. **Journal of Biological Chemistry**, v. 275, n. 51, p. 40517-40528, 2000.

ISHIDA, M. et al. Solvent- and mechanical-treatment-induced conformational transition of silk fibroins studied by high. **Macromolecules**, v. 94, n. 37, p. 88-94, 1990.

JIMENEZ-VILLAR, E. et al. Novel core-shell ($\text{TiO}_2@$ silica) nanoparticles for scattering medium in a random laser: higher efficiency, lower laser threshold and lower photodegradation. **Nanoscale**, v. 5, n. 24, p. 12512-12517, 2013.

JIN, H.-J.; KAPLAN, D. L. Mechanism of silk processing in insects and spiders. **Nature**, v. 424, n. 6952, p. 1057-1061, 2003.

JIN, H.- J. et al. Water-stable silk films with reduced β -sheet content. **Advanced Functional Materials**, v. 15, n. 8, p. 1241-1247, 2005.

KAPLAN, D. et al. Silk. In: KAPLAN, D.; McGRATH, K. (Ed.). **Protein-based materials**. Boston: Birkhäuser, 2012. Chap. 4, p. 103-133.

KELLY, J. A. et al. The development of chiral nematic mesoporous materials. **Accounts of Chemical Research**, v. 47, n. 4, p. 1088-1096, 2014.

KHAN, M. K. et al. Flexible mesoporous photonic resins with tunable chiral nematic structures. **Angewandte Chemie International Edition**, v. 52, n. 34, p. 8921-8924, 2013.

KIKUCHI, H. et al. Polymer-stabilized liquid crystal blue phases. **Nature Materials**, v. 1, n. 1, p. 64-68, Sept. 2002.

KIM, D.-H. et al. Dissolvable films of silk fibroin for ultrathin conformal bio-integrated electronics. **Nature Materials**, v. 9, n. 6, p. 511-517, 2010.

KIM, S. et al. Silk inverse opals. **Nature Photonics**, v. 6, n. 12, p. 818-823, 2012.

KIM, U. J. et al. Structure and properties of silk hydrogels. **Biomacromolecules**, v. 5, n. 3, p. 786-792, 2004.

KIRK, A. G.; ANDREWS, M. P. Nanocrystalline cellulose for covert optical encryption. **Journal of Nanophotonics**, v. 6, n. 1, p. 63511-63516, 2012.

KISHIMOTO, Y. et al. Nanocomposite of silk fibroin nanofiber and montmorillonite: fabrication and morphology. **International journal of biological macromolecules**, v. 57, p. 124-128, 2013.

- KLEMM, D. et al. Cellulose: fascinating biopolymer and sustainable raw material. **Angewandte Chemie International Edition**, v. 44, n. 22, p. 3358-3393, 2005.
- KLEMM, D. et al. Nanocelluloses: a new family of nature-based materials. **Angewandte Chemie International Edition**, v. 50, n. 24, p. 5438-5466, 2011.
- KODAMA, K. The preparation and physico-chemical properties of sericin. **Biochemical Journal**, v. 20, n. 6, p. 1208-1222, 1926.
- KOH, L. D. et al. Structures, mechanical properties and applications of silk fibroin materials. **Progress in Polymer Science**, v. 46, p. 86-110, 2015.
- KONDO, T.; SAWATARI, C. A fourier transform infra-red spectroscopic analysis of the character of hydrogen bonds in amorphous cellulose. **Polymer**, v. 37, n. 3, p. 393-399, 1996.
- KOPP, V. I. et al. Low-threshold lasing at the edge of a photonic stop band in cholesteric liquid crystals. **Optics Letters**, v. 23, n. 21, p. 1707-1709, 1998.
- KUNDU, B. et al. Silk fibroin biomaterials for tissue regenerations. **Advanced Drug Delivery Reviews**, v. 65, n. 4, p. 457-470, 2013.
- LAGERWALL, J. P. F. et al. Cellulose nanocrystal-based materials: from liquid crystal self-assembly and glass formation to multifunctional thin films. **NPG Asia Materials**, v. 6, n. 1, 2014. doi:10.1038/am.2013.69.
- LEGNANI, C. et al. Bacterial cellulose membrane as flexible substrate for organic light emitting devices. **Thin Solid Films**, v. 517, n. 3, p. 1016-1020, 2008.
- LETOKHOV, V. S. Stimulated emission of an ensemble of scattering particles with negative absorption. **ZhETF Pisma Redaktsiiu**, v. 5, p. 212-215, 1967.
- LI, X. et al. In situ synthesis of CdS nanoparticles on bacterial cellulose nanofibers. **Carbohydrate Polymers**, v. 76, n. 4, p. 509-512, 2009.
- LIMA, L. R. et al. Silk fibroin-antigenic peptides-YVO₄:Eu³⁺ nanostructured thin films as sensors for hepatitis C. **Journal of Luminescence**, v. 170, p. 375-379, 2016.
- LIN, N.; DUFRESNE, A. Nanocellulose in biomedicine: current status and future prospect. **European Polymer Journal**, v. 59, p. 302-325, 2014.
- LIPPMAA, E. et al. Structural studies of silicates by solid-state high-resolution ²⁹Si NMR. **Journal of the American Chemical Society**, v. 102, n. 15, p. 4889-4893, 1980.
- LIU, L. et al. Mesoporous hybrid from anionic polyhedral oligomeric silsesquioxanes (POSS) and cationic surfactant by hydrothermal approach. **Microporous and Mesoporous Materials**, v. 132, p. 567-571, 2010.
- LIU, X.; ZHANG, K. Silk fiber - molecular formation mechanism, structure-property relationship and advanced applications. In: LESIER, C. (Ed.). **Oligomerization of chemical and biological compounds**. Rijeka: Intech, 2014. Chap. 3, p. 69-102.

- LOFAJ, M.; VALENT, I.; BUJDAK, J. Mechanism of rhodamine 6G molecular aggregation in montmorillonite colloid. **Open Chemistry**, v. 11, n. 10, p. 1606-1619, 2013.
- LOWELL, S. et al. **Characterization of porous solids and powders: surface area, pore size and density**. Dordrecht: Springer, 2004.
- LUAN, F. et al. Lasing in nanocomposite random media. **Nano Today**, v. 10, n. 2, p. 168-192, 2015.
- LUO, K.; YANG, Y.; SHAO, Z. Physically crosslinked biocompatible silk-fibroin-based hydrogels with high mechanical performance. **Advanced Functional Materials**, p. 872-880, 2015.
- MANNING, A. P. et al. NMR of guest-host systems: 8CB in chiral nematic porous glasses. **Magnetic Resonance in Chemistry**, v. 52, n. 10, p. 532-539, 2014.
- MARCHESSAULT, R. H.; MOREHEAD, F. F.; WALTER, N. M. Liquid crystal systems from fibrillar polysaccharides. **Nature**, v. 184, n. 4686, p. 632-633, 1959.
- MARELLI, B. et al. Silk fibroin as edible coating for perishable food preservation. **Scientific Reports**, v. 6, 2016. doi:10.1038/srep25263.
- MARKUSHEV, V. M.; ZOLIN, V. F.; BRISKINA, C. M. Luminescence and stimulated emission of neodymium in sodium lanthanum molybdate powders. **Quantum Electronics**, v. 16, n. 2, p. 281-283, 1986.
- MARSH, R. E.; COREY, R. B.; PAULING, L. An investigation of the structure of silk fibroin. **Biochimica et Biophysica Acta**, v. 16, p. 1-34, 1955.
- MARTÍNEZ, V. M. et al. Characterization of rhodamine 6G aggregates intercalated in solid thin films of laponite clay . 1 . Absorption spectroscopy characterization of rhodamine 6G aggregates intercalated in solid thin films of laponite. **Journal Physical Chemistry B**, v. 109, p. 7443-7450, 2005.
- MATOS, C. J. S. de et al. Random fiber laser. **Physical Review Letters**, v. 99, n. 15, p. 153903/1-153903/4, 2007.
- MATSUMOTO, A. et al. Mechanisms of silk fibroin sol-gel transitions. **Journal of Physical Chemistry B**, v. 110, n. 43, p. 21630-21638, 2006.
- MENEZES, A. J. de et al. Extrusion and characterization of functionalized cellulose whiskers reinforced polyethylene nanocomposites. **Polymer**, v. 50, n. 19, p. 4552-4563, 2009.
- MIESZAWSKA, A. J. et al. Osteoinductive silk-silica composite biomaterials for bone regeneration. **Biomaterials**, v. 31, n. 34, p. 8902-8910, 2010.
- MONTI, P. et al. Raman spectroscopic characterization of *Bombyx mori* silk fibroin: Raman spectrum of silk I. **Journal of Raman Spectroscopy**, v. 32, p. 103-107, 2001.

MOON, R. J. et al. Cellulose nanomaterials review: structure, properties and nanocomposites. **Chemical Society Reviews**, v. 40, n. 7, p. 3941-3994, 2011.

MORI, H.; TSUKADA, M. New silk protein: modification of silk protein by gene engineering for production of biomaterials. **Reviews in Molecular Biotechnology**, v. 74, n. 2, p. 95-103, 2000.

MOTTA, A.; FAMBRI, L.; MIGLIARESI, C. Regenerated silk fibroin films: thermal and dynamic mechanical analysis. **Spectrum**, v. 203, p. 1658-1665, 2002.

MOURA, A. L. et al. Multi-wavelength emission through self-induced second-order wave-mixing processes from a Nd³⁺ doped crystalline powder random laser. **Scientific Reports**, v. 5, 2015. doi:10.1038/srep13816.

NAGARKAR, S. et al. Structure and gelation mechanism of silk hydrogels. **Physical Chemistry Chemical Physics**, v. 12, n. 15, p. 3834-3844, 2010.

NELSON, D. L.; COX, M. M. **Princípios de bioquímica de Lehninger**. Porto Alegre: Artmed, v. 6, 2011.

NGUYEN, T.; HAMAD, W. Y.; MacLACHLAN, M. J. CdS quantum dots encapsulated in chiral nematic mesoporous silica : New iridescent and luminescent Materials. **Advanced Functional Materials**, v. 24, p. 777-783, 2014.

NOGINOV, M. A. Other types of solid-state random lasers. In: _____. **Solid-state random lasers**. New York: Springer, 2005. Chap. 9, p. 198-221. (Springer series in optical sciences, v. 105).

NUMATA, K.; CEBE, P.; KAPLAN, D. L. Mechanism of enzymatic degradation of beta-sheet crystals. **Biomaterials**, v. 31, n. 10, p. 2926-2933, 2010.

OH, S. Y. et al. Crystalline structure analysis of cellulose treated with sodium hydroxide and carbon dioxide by means of X-ray diffraction and FTIR spectroscopy. **Carbohydrate Research**, v. 340, n. 15, p. 2376-2391, 2005.

OHZONO, T.; YAMAMOTO, T.; FUKUDA, J. A liquid crystalline chirality balance for vapours. **Nature Communications**, v. 5, 2014. doi:10.1038/ncomms4735.

OMENETTO, F. G.; KAPLAN, D. L. A new route for silk. **Nature Photonics**, v. 2, n. 11, p. 641-643, 2008.

OMENETTO, F. G.; KAPLAN, D. L. New opportunities for an ancient material. **Science**, v. 329, n. 5991, p. 528-531, 2010.

PAN, J.; HAMAD, W.; STRAUS, S. K. Parameters affecting the chiral nematic phase of nanocrystalline cellulose films. **Macromolecules**, v. 43, n. 8, p. 3851-3858, 2010.

PENNINCK, L. et al. Light emission from dye-doped cholesteric liquid crystals at oblique angles: simulation and experiment. **Physical Review E: Statistical, Nonlinear, and Soft Matter Physics**, v. 85, n. 4, pt. 1, p. 041702/1-041702/7, 2012.

PENNISI, E. Diverse crystals account for beetle sheen. **Science**, v. 341, n. 6142, p. 120, 2013.

PEREIRA, C. et al. Copper acetylacetonate anchored onto amine-functionalised clays. **Journal of Colloid and Interface Science**, v. 316, n. 2, p. 570-579, 2007.

PEREIRA, R. F. P.; SILVA, M. M.; DE ZEA BERMUDEZ, V. *Bombyx mori* silk fibers: an outstanding family of materials. **Macromolecular Materials and Engineering**, v. 300, n. 12, p. 1171-1198, 2015.

PING, Y. et al. Structured color humidity indicator from reversible pitch tuning in self-assembled nanocrystalline cellulose films. **Sensors & Actuators B: Chemical**, v. 176, p. 692-697, 2013.

PINTO, E. R. P. et al. Transparent composites prepared from bacterial cellulose and castor oil based polyurethane as substrates for flexible OLEDs. **Journal of Materials Chemistry C**, v. 3, n. 44, p. 11581-11588, 2015.

PIRANI, S.; HASHAIKEH, R. Nanocrystalline cellulose extraction process and utilization of the byproduct for biofuels production. **Carbohydrate Polymers**, v. 93, n. 1, p. 357-363, 2013.

PREDA, R. C. et al. Bioengineered silk proteins to control cell and tissue functions. In: GERRARD, J. A. (Ed.). **Protein nanotechnology: protocols, instrumentation, and applications**. 2nd ed. New York: Humana Press, 2013. p. 19-41. (Methods in molecular biology, v. 996).

PROUZET, E. et al. Roughness of mesoporous silica surfaces deduced from adsorption measurements. **Microporous and Mesoporous Materials**, v. 119, p. 9-17, 2009.

QIU, K.; NETRAVALI, A. N. A Review of fabrication and applications of bacterial cellulose based nanocomposites. **Polymer Reviews**, v. 54, n. 4, p. 598-626, 2014.

QU, D. et al. Chiral fluorescent films of gold nanoclusters and photonic cellulose with modulated fluorescence emission. **Journal Material Chemistry C**, v. 4, n. 9, p. 1764-1768, 2016.

QUEREJETA-FERNÁNDEZ, A. et al. Chiral plasmonic films formed by gold nanorods and cellulose nanocrystals. **Journal of the American Chemical Society**, v. 136, p. 4788-4793, 2014.

QUEREJETA-FERNANDEZ, A. et al. Circular dichroism of chiral nematic films of cellulose nanocrystals loaded with plasmonic nanoparticles. **ACS Nano**, v. 9, n. 10, p. 10377-10385, 2015.

RÅNBY, B. G. Fibrous macromolecular systems. Cellulose and muscle. The colloidal properties of cellulose micelles. **Discussions of the Faraday Society**, v. 11, p. 158-164, 1951.
REDDING, B.; CHOMA, M. A.; CAO, H. Speckle-free laser imaging using random laser illumination. **Nature Photonics**, v. 6, n. 6, p. 355-359, 2012.

REVOL, J. et al. Helicoidal self-ordering of cellulose microfibrils in aqueous suspension. **International Journal of Biological Macromolecules**, v. 14, p. 170-172, 1992.

REVOL, J.-F.; GODBOUT, L.; GRAY, D. G. Solid self-assembled films of cellulose with chiral nematic order and optically variable properties. **Journal of Pulp and Paper Science**, v. 24, n. 5, p. 146-149, 1998.

ROCHA, L. A. et al. Luminescence properties of Eu-complex formations into ordered mesoporous silica particles obtained by the spray pyrolysis process. **Nanotechnology**, v. 26, n. 33, p. 335604/1-335604/11, 2015.

ROMAN, M.; WINTER, W. T. Effect of sulfate groups from sulfuric acid hydrolysis on the thermal degradation behavior of bacterial cellulose. **Biomacromolecules**, v. 5, p. 1671-1677, 2004.

SAITÔ, H. et al. High-resolution ¹³C NMR study of silk fibroin in the solid state by the cross-polarization-magic angle spinning method. Conformational characterization of silk I and silk II type forms of *Bombyx mori* fibroin by the conformation-dependent ¹³C chemical shift. **Macromolecules**, v. 17, n. 35, p. 1405-1412, 1984.

SAITO, T. et al. Cellulose nanofibers prepared by TEMPO-mediated oxidation of native cellulose. **Biomacromolecules**, v. 8, n. 8, p. 2485-2491, 2007.

SALAJKOVÁ, M.; BERGLUND, L. A.; ZHOU, Q. Hydrophobic cellulose nanocrystals modified with quaternary ammonium salts. **Journal of Materials Chemistry**, v. 22, n. 37, p. 19798-19805, 2012.

SANTOS, M. V. dos et al. Random laser action from flexible biocellulose-based device. **Journal of Applied Physics**, v. 115, n. 8, p. 083108/1-083108/5, 2014.

SHAH, N. et al. Overview of bacterial cellulose composites: a multipurpose advanced material. **Carbohydrate Polymers**, v. 98, n. 2, p. 1585-1598, 2013.

SHIMURA, K. et al. Studies on silk fibroin of *Bombyx mori*. I. Fractionation of fibroin prepared from the posterior silk gland. **Journal of biochemistry**, v. 80, n. 4, p. 693-702, 1976.

SHIN, Y.; EXARHOS, G. J. Template synthesis of porous titania using cellulose nanocrystals. **Materials Letters**, v. 61, n. 11, p. 2594-2597, 2007.

SHOPSOWITZ, K. E.; HAMAD, W. Y.; MacLACHLAN, M. J. Chiral nematic mesoporous carbon derived from nanocrystalline cellulose. **Angewandte Chemie International Edition**, v. 50, n. 46, p. 10991-10995, 2011.

SHOPSOWITZ, K. E.; HAMAD, W. Y.; MacLACHLAN, M. J. Flexible and iridescent chiral nematic mesoporous organosilica films. **Journal of the American Chemical Society**, v. 134, n. 2, p. 867-870, 2012.

SHOPSOWITZ, K. E. et al. Free-standing mesoporous silica films with tunable chiral nematic structures. **Nature**, v. 468, n. 7322, p. 422-425, 2010.

SHOPSOWITZ, K. E. et al. Hard templating of nanocrystalline titanium dioxide with chiral nematic ordering. **Angewandte Chemie International Edition**, v. 51, n. 28, p. 6886-6890, 2012.

SHOPSOWITZ, K. E. et al. Biopolymer templated glass with a twist: controlling the chirality, porosity, and photonic properties of silica with cellulose nanocrystals. **Advanced Functional Materials**, v. 24, n. 3, p. 327-338, 2014.

SILVA, R. R. da et al. Silk fibroin biopolymer films as efficient hosts for DFB laser operation. **Journal of Materials Chemistry C**, v. 1, n. 43, p. 7181-7190, 2013.

SIQUEIRA, G.; BRAS, J.; DUFRESNE, A. Cellulose whiskers versus microfibrils: influence of the nature of the nanoparticle and its surface functionalization on the thermal and mechanical properties of nanocomposites. **Biomacromolecules**, v. 10, p. 425-432, 2009.

SMITH, M. A.; LOBO, R. F. A fractal description of pore structure in block-copolymer templated mesoporous silicates. **Microporous and Mesoporous Materials**, v. 131, p. 204-209, 2010.

STEINER, U.; VIGNOLINI, S. Digital color in cellulose nanocrystal films. **ACS Applied Materials and Interfaces**, v. 6, n. 15, p. 12302-12306, 2014.

SULAEVA, I. et al. Bacterial cellulose as a material for wound treatment: properties and modifications. A review. **Biotechnology Advances**, v. 33, n. 8, p. 1547-1571, 2015.

SZNITKO, L.; MYSLIWIEC, J.; MINIEWICZ, A. The role of polymers in random lasing. **Journal of Polymer Science, Part B: Polymer Physics**, v. 53, n. 14, p. 951-974, 2015.

TANAKA, K.; INOUE, S.; MIZUNO, S. Hydrophobic interaction of P25, containing Asn-linked oligosaccharide chains, with the HL complex of silk fibroin produced by *Bombyx mori*. **Insect Biochemistry and Molecular Biology**, v. 29, n. 3, p. 269-276, 1999.

TANAKA, K. et al. Determination of the site of disulfide de linkage between heavy and light chains of silk fibroin produced by *Bombyx mori*. **Science**, v. 1432, p. 92-103, 1999.

TAO, H.; KAPLAN, D. L.; OMENETTO, F. G. Silk materials - a road to sustainable high technology. **Advanced Materials**, v. 24, p. 2824-2837, 2012.

TAO, H. et al. Inkjet Printing of regenerated silk fibroin: from printable forms to printable functions. **Advanced Materials**, v. 27, n. 29, p. 4273-4279, 2015.

TERCJAK, A.; GUTIERREZ, J. Conductive properties of photoluminescent Au/Ps-b-PEO inorganic/organic hybrids containing nematic liquid crystals. **The Journal of Physical Chemistry C**, v. 115, n. 5, p. 1643-1648, 2011.

TERCJAK, A.; GARCIA, I.; MONDRAGON, I. Liquid crystal alignment in electro-responsive nanostructured thermosetting materials based on block copolymer dispersed liquid crystal. **Nanotechnology**, v. 19, n. 27, p. 275701/1- 275701/5, 2008.

TERCJAK, A. et al. Polymer dispersed liquid crystals based on poly(styrene-b-ethylene oxide), poly(bisphenol a carbonate) or poly(methylphenylsiloxane), and 4'-(hexyloxy)-4-biphenyl-carbonitrile: analysis of phase diagrams and morphologies generated. **Journal of Applied Polymer Science**, v. 108, n. 2, p. 1116-1125, 2008.

TERCJAK, A. et al. Thermoresponsive inorganic/organic hybrids based on conductive TiO₂ nanoparticles embedded in poly (styrene-b-ethylene oxide) block copolymer dispersed liquid crystals. **Acta Materialia**, v. 57, n. 15, p. 4624-4631, 2009.

TERCJAK, A. et al. Conductive properties of switchable photoluminescence thermosetting systems based on liquid crystals. **Langmuir**, v. 26, n. 6, p. 4296-302, 2010.

TERCJAK, A. et al. Nano- and macroscale structural and mechanical properties of in situ synthesized bacterial cellulose/PEO-\nb\n-PPO-\nb\n-PEO biocomposites. **ACS Applied Materials & Interfaces**, v. 7, n. 7, p. 4142-4150, 2015.

TERCJAK, A. et al. Switchable photoluminescence liquid crystal coated bacterial cellulose films with conductive response. **Carbohydrate Polymers**, v. 143, p. 188-197, 2016.

TRÉBOSC, J. et al. Solid-state NMR study of MCM-41-type mesoporous silica nanoparticles. **Journal of the American Chemical Society**, v. 127, n. 9, p. 3057-3068, 2005.

UNGER, K. K.; SKUDAS, R.; SCHULTE, M. M. Particle packed columns and monolithic columns in high-performance liquid chromatography-comparison and critical appraisal. **Journal of Chromatography A**, v. 1184, n. 1/2, p. 393-415, 2008.

VALLUZZI, R. et al. Orientation of silk III at the air-water interface. **International Journal of Biological Macromolecules**, v. 24, n. 2, p. 237-242, 1999.

VAN OPDENBOSCH, B. D.; ZOLLFRANK, C. Cellulose-based biotemplated silica. **Advanced Engineering Materials**, v. 16, n. 6, p. 699-712, 2014.

VAVELIUK, P.; SILVA, A. M. de B.; OLIVEIRA, P. C. de. Model for bichromatic laser emission from a laser dye with nanoparticle scatterers. **Physical Review A**, v. 68, n. 1, p. 13805/1-13805/9, 2003.

VEPARI, C.; KAPLAN, D. L. Silk as a biomaterial. **Progress in Polymer Science**, v. 32, n. 8/9, p. 991-1007, 2007.

VOLLRATH, F.; PORTER, D. Silks as ancient models for modern polymers. **Polymer**, v. 50, n. 24, p. 5623-5632, 2009.

WANG, C.; HSIEH, C.; HWANG, J. Flexible organic thin-film transistors with silk fibroin as the gate dielectric. **Advanced Materials**, v. 23, n. 14, p. 1630-1634, 2011.

WANG, H. et al. A study on the flow stability of regenerated silk fibroin aqueous solution. **International Journal of Biological Macromolecules**, v. 36, n. 1, p. 66-70, 2005.

- WANG, H. Y.; CHEN, Y. Y.; ZHANG, Y. Q. Processing and characterization of powdered silk micro- and nanofibers by ultrasonication. **Materials Science and Engineering C**, v. 48, p. 444-452, 2015.
- WANG, Y.; XU, Y. Chiral nematic mesoporous films of $ZrO_2:Eu^{3+}$: new luminescent materials. **Dalton Transactions**, v. 43, n. 41, p. 15321-15327, 2014.
- WEAVER, J. C. et al. The stomatopod dactyl club: a formidable damage-tolerant biological hammer. **Science**, v. 336, n. 6086, p. 1275-1280, 2012.
- WHITE, J. L.; WANG, X. Structural investigations of solid proteins at natural abundance using. **Macromolecules**, v. 35, p. 2633-2639, 2002.
- WU, Z. et al. Bacterial cellulose: a robust platform for design of three dimensional carbon-based functional nanomaterials. **Accounts of Chemical Research**, v. 49, n. 1, p. 96-105, 2015.
- XU, Q. et al. Novel and simple synthesis of hollow porous silica fibers with hierarchical structure using silk as template. **Materials Science and Engineering: B**, v. 127, n. 2, p. 212-217, 2006.
- YAMAGUCHI, K. et al. Primary structure of the silk fibroin light chain determined by cDNA sequencing and peptide analysis. **Journal of Molecular Biology**, v. 210, n. 1, p. 127-139, 1989.
- YANG, D. et al. Control of reflectivity and bistability in displays using cholesteric liquid-crystals. **Journal of Applied Physics**, v. 76, n. 2, p. 1331-1333, 1994.
- YANG, W. et al. Natural flexible dermal armor. **Advanced Materials**, v. 25, n. 1, p. 31-48, 2013.
- YASHCHUK, V. P. Coupled effect of stimulated Raman scattering and random lasing of dyes in multiple scattering medium. **Laser Physics**, v. 25, n. 7, p. 75702/1-75702/6, 2015.
- YASHCHUK, V. P. et al. Stimulated Raman scattering of laser dye mixtures dissolved in multiple scattering media. **Quantum Electronics**, v. 44, n. 10, p. 921, 2014.
- ZHANG, J. et al. Silkworm cocoon as natural material and structure for thermal insulation. **Materials and Design**, v. 49, p. 842-849, 2013.
- ZHANG, Y. P. et al. Structured color humidity indicator from reversible pitch tuning in self-assembled nanocrystalline cellulose films. **Sensors and Actuators, B: Chemical**, v. 176, p. 692-697, 2013.
- ZHANG, Y.-Q. Applications of natural silk protein sericin in biomaterials. **Biotechnology Advances**, v. 20, n. 2, p. 91-100, 2002.
- ZHAO, J. et al. Apatite-coated silk fibroin scaffolds to healing mandibular border defects in canines. **Bone**, v. 45, n. 3, p. 517-527, 2009.

ZHENG, J.; ZHANG, C.; DICKSON, R. M. Highly fluorescent, water-soluble, size-tunable gold quantum dots. **Physical Review Letters**, v. 93, n. 7, p. 77402/1-77402/2, 2004.

ZHOU, C. et al. Silk fibroin: structural implications of a remarkable amino acid sequence. **Proteins: Structure, Function, and Bioinformatics**, v. 44, n. 2, p. 119-122, 2001.

ZHOU, J. et al. Control of the anchoring behavior of polymer-dispersed liquid crystals: effect of branching in the side chains of polyacrylates. **Journal of the American Chemical Society**, v. 124, p. 9980-9981, 2002.

ZHOU, P. et.al. Structure of *Bombyx mori* silk fibroin based on the DFT chemical shift calculation. **The Journal of Physical Chemistry B**, v. 105, n.50, p. 12469-12476, 2001.

ZHOU, Y.; DING, E.-Y.; LI, W.-D. Synthesis of TiO₂ nanocubes induced by cellulose nanocrystal (CNC) at low temperature. **Materials Letters**, v. 61, n. 28, p. 5050-5052, 2007.